Evaluation of EURIPIDES pile load tests response from CPT data

Fawad S. Niazi, *Research Assistant, Geosystems Engrg. Div., School of Civ. & Environ. Engrg., Georgia Institute of Technology, 790 Atlantic Drive, Atlanta, GA 30332, USA; e-mail: fniazi6@gatech.edu*
Paul W. Mayne, *Professor, Geosystems Engrg. Div., School of Civ. & Environ. Engrg., Georgia Institute of Technology, 790 Atlantic Drive, Atlanta, GA, 30332 USA; e-mail: paul.mayne@ce.gatech.edu*

ABSTRACT: *Cone penetration tests (CPT) are used to evaluate the nonlinear axial load-displacement-capacity performance of a large driven pile from the EURIPIDES project. The 0.76-m diameter pile was driven open-ended in dense sands at Eemshaven, The Netherlands, and tested in static compression and tension at three successive penetration depths: 30.5m, 38.7m and 47.0m. The profiles of four independent readings with depth [total tip resistance (q_t), sleeve friction (f_s), mid-face porewater (u_1) pressure, and shear wave velocity (V_s)], provided by seismic piezocone tests (SCPTu) were utilized to evaluate the soil engineering parameters at the site. These parameters were employed in a rational manner for the axial capacity evaluations. Other direct CPT methods that allow the SCPTu readings for pile capacity evaluations were also utilized to obtain unit pile side friction (f_p) and end bearing (q_b). The V_s readings enable the determination of the small strain shear modulus (G_{max}) profile that provides the initial fundamental stiffness for the axial load-settlement response by integrating the elastic continuum solution and modulus reduction curves.*

KEYWORDS: Pile foundation, seismic piezocone tests, settlement, axial pile capacity, pile load test

SITE LOCATION: IJGCH-database.kmz (requires Google Earth)

INTRODUCTION

An extensive axial pile load testing program was conducted under a joint industry project by Fugro Engineers of The Netherlands and Geodia S.A. of France on a highly-instrumented 0.76m outer diameter pipe pile driven open-ended in very dense sands at Eemshaven, The Netherlands (see Figure 1). The project is known as EURIPIDES (European initiative on piles in dense sands), and the pile load tests were performed to obtain reliable data in order to improve offshore pile design criteria (Fugro 2004). The program consisted of a series of static compression, tension and cyclic load tests. For the program, the pile was driven and tested at three penetration depths. Detailed information on the EURIPIDES program, equipment, instrumentation and results has previously been published (e.g., Zuidberg and Vergobbi 1996, Fugro 2004, Kolk et al. 2005). Subsequent to the program, a number of researchers have used several CPT-based pile capacity design methods to predict the pile load test results (e.g. Jardine et al. 2005, Lehane et al. 2005a, Schneider et al. 2008).

This paper briefly reviews the geotechnical site characterization using the results of in situ tests and then applies several CPT methods to predict the pile load tests results. An evaluation of the axial load carrying capacity and the load-displacement response is presented using information from SCPTu conducted at the site.

In contrast to the earlier prediction studies for this site, the unique aspects presented in this paper are enumerated below:

- Several CPT direct and indirect methods for pile capacity evaluation that have not previously been used or presented with the EURIPIDES data (Kajima Technical Research Institute (KTRI) method, Laboratoire Central des Ponts et Chaussées (LCPC) method, UNICONE method, limit plasticity method, and beta (β) method) were applied for this study.

- This paper presents new data, specifically a complete SCPTu sounding that includes: q_c, f_s, u_1 and V_s readings with depth that was provided by Fugro Engineers. All earlier studies considered only the measured tip resistance (q_c) based CPT methods for capacity evaluations.

- Complete interpretations of relevant geotechnical engineering parameters using SCPTu-based correlations are presented.

- The shear wave velocity (V_s) profile has been utilized to obtain the profile of G_{max} at this site. The evaluation of the nonlinear axial load-displacement response is found by integrating the elastic continuum solution proposed by Randolph and Wroth (1978, 1979) and the algorithm proposed by Fahey and Carter (1993) for reducing G_{max} at increasing load levels.

A very concise overview of the test program has also been included in the 'Test Site' and 'Load Test Program' sections in order to develop understanding of the site and the test program. The information given in this overview was collected from the earlier published documents (Zuidberg and Vergobbi 1996, Fugro 2004, and Kolk et al. 2005). It is pointed that all the field and laboratory investigations for this project were conducted by the Fugro and Geodia teams and additional details are given elsewhere.
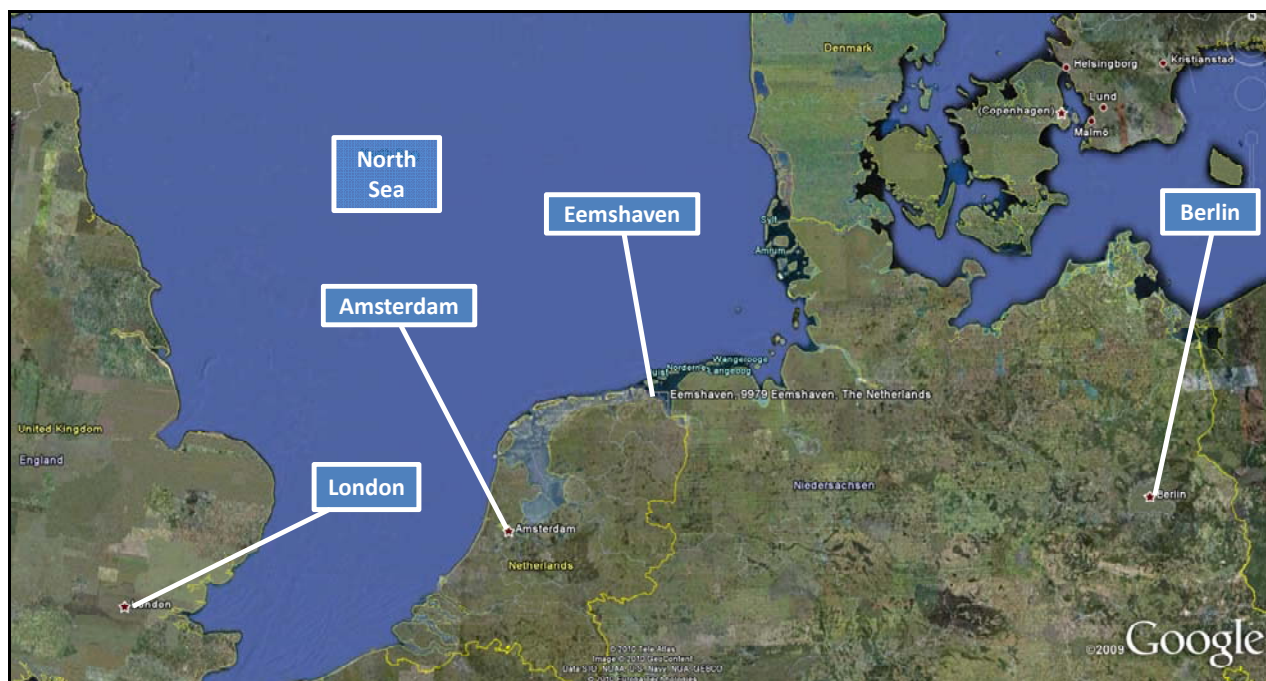

Figure 1. Location of EURIPIDES project site at Eemshaven, The Netherlands (Google Map 2009).

TEST SITE

The EURIPIDES project site was investigated and characterized based on data and information obtained from 3 boreholes (BH), 7 cone penetration tests (CPT), 2 seismic piezocone tests (SCPTu), and associated laboratory tests on retrieved soil samples, including: classification, grain size analysis, dry density measurement, triaxial shear test, direct shear test, and consolidation test (Zuidberg and Vergobbi 1996).

The measured penetrometer readings from all the CPT soundings portrayed similar profiles with depth and the profiles from SCPTu-36 sounding showing typical results are presented in Figure 2. SCPTu-36 was the deepest sounding and it was closest to the nearby borehole at the site. The interpreted soil conditions from the borehole are also shown in Figure 2. The soil profile consists of a sequence of Holocene and Pleistocene fine to medium sands (loose to very dense) extending from the water table (1.5m below ground level (bgl)) to in excess of 50 m (except for layers containing inclusions of soft clay and silt). These soils are overlain by about 5m of man-made fill ground. The fill and loose Holocene sands extend to

about 22 m depth with an average measured tip resistance (q_c) of about 5.8 MPa. Below that depth, q_c values varied between 20 and 90 MPa from different CPT soundings (Zuidberg and Vergobbi 1996; Fugro 2004). Dense Pleistocene sand, occurring below 25 m depth, has been subjected to multiple glaciations, resulting in overconsolidation (Zuidberg and Vergobbi 1996, and Fugro 2004). These profiles have also been confirmed from the soil behavior type (SBT) classification index (I_c) and the relative density (D_R) evaluations using the CPT-based correlations (shown later in this paper). The state of denseness was based on the D_R criteria presented in Holtz (1973).
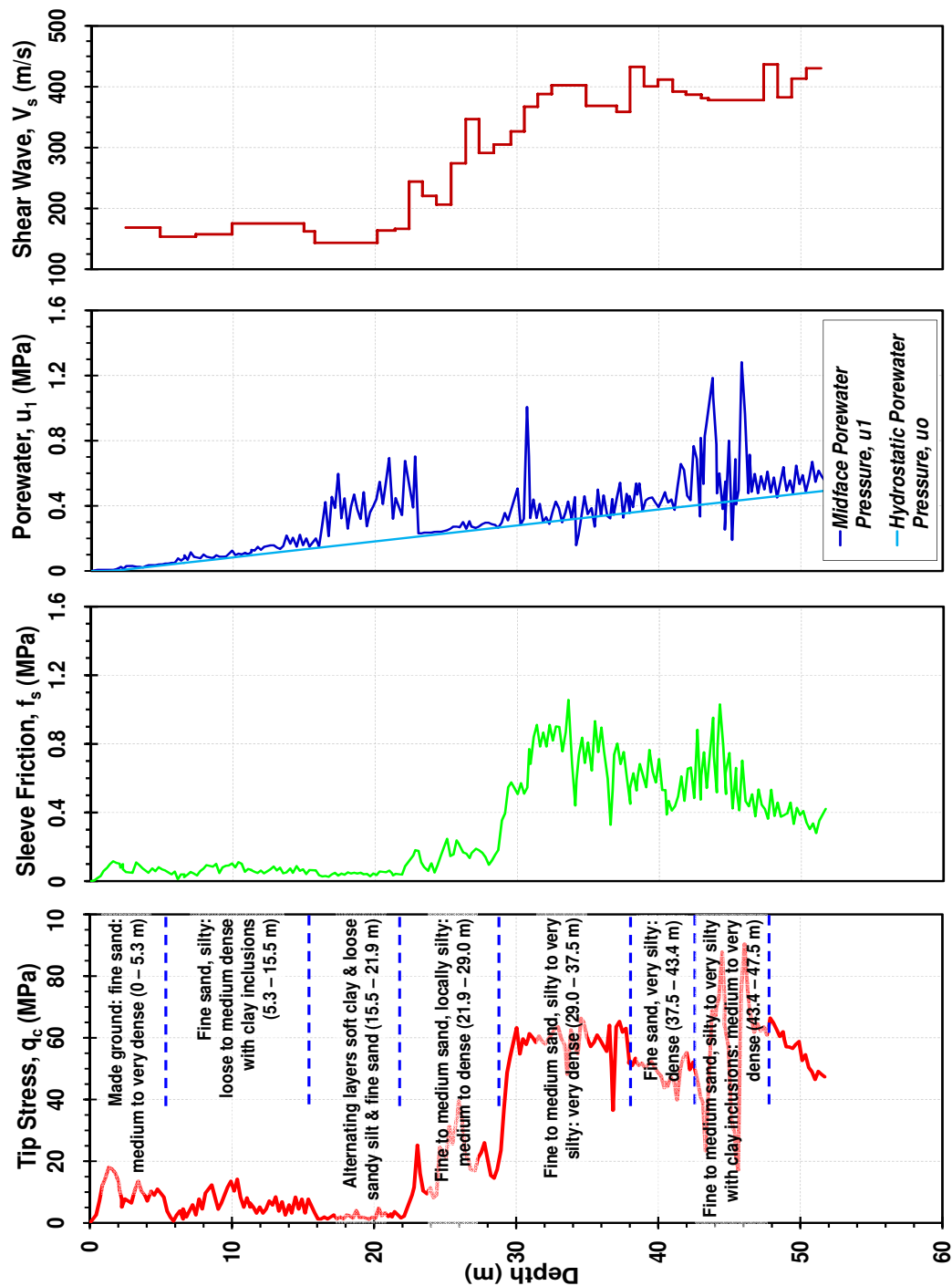

Figure 2. Seismic piezocone test 36 sounding profiles at location 1 of EURIPIDES project (after Fugro 2004).

The soil profiles and the related geotechnical parameters thus obtained have been used in this study for the response evaluation of the pile tested at multiple depths.

LOAD TEST PROGRAM

Test Pile

Fugro engineers designed and conducted the pile load tests to provide pile-soil interaction data on the test sands below 22 m. Accordingly, the test pile consisted of a 27 m long instrumented lower section and a 22 m long upper section. The instrumented section had a wall thickness of 35 mm and a pile axial stiffness modulus, E_p of 37,500 MPa. In order for the pile to sustain the maximum anticipated axial compression stress (375 MPa) and the driving stresses without fatigue damage, the steel type selected for the test pile had a minimum yield stress of 450 MPa. The add-on section had a wall thickness of 41 mm in order to provide sufficient bending resistance in the upper soils (Zuidberg and Vergobbi 1996). The key instrumentation mounted at various levels along the instrumented section included: axial and (limited) tangential strain gauges, total pressure cells, porewater pressure cells, toe load cells, and thermocouples.

Load Tests

The pile was load tested in compression (C) and tension (T) after each successive driving to depths of 30.5 m, 38.7 m and 47.0 m. All load tests were performed at a constant rate of displacement of 1 mm/minute. Tension tests were continued to failure or a pile head displacement of 75 mm, whichever occurred first. For compression tests, loading continued until a head displacement of 190 mm was achieved.

Measurements obtained during testing included load-displacement at the pile head, pile toe and at 22m pile embedment depth, frictional resistance along the outside pile shaft, and end bearing. The toe load cells were damaged during pile driving (Fugro 2004). Pile tip forces were, therefore, calculated using results from the strain gauge closest to the pile toe (i.e. 0.38 m above the pile tip). For this study, results from compression load tests (presented later) were selected for comparison with the analysis based on SCPTu-36.

CPT METHODS FOR PILE RESPONSE EVALUATION

The seismic piezocone test (SCPTu) is a quick, reliable and economical in situ hybrid test that provides downhole measurements of V_s in addition to the penetration test parameters of q_c, f_s, and u_1 and/or u_2 within a single vertical sounding. These parameters can be utilized to obtain very detailed stratigraphic information in terms of soil classification and soil engineering properties. The analysis of pile foundations can be performed using geotechnical properties evaluated from the SCPTu readings. The penetrometer readings facilitate assessment of the peak strength on the stress-strain-strength curves corresponding to the pile capacity. Downhole geophysics (in terms of V_s) are used to calculate G_{max}, or equivalent Young's Modulus (E_{max}), corresponding to the initial soil deformation ($\gamma_s < 10^{-6}$) on the stress-strain-strength curve. These results, applied within elasticity theory (Fleming et al. 1992; Poulos and Davis 1980; Randolph and Wroth 1978, 1979), can be used to predict the entire axial load-displacement-capacity behavior of deep foundations. With this approach, the SCPTu readings are used to classify soil types, calculate soil engineering parameters, and predict pile response in terms of axial load-displacement-capacity.

Soil Classification

Amongst CPT based soil classification methods, the charts using soil behavioral type (SBT) are based on normalized CPT parameters proposed by Jefferies and Davis (1991). The CPT material index I_c identified by Jefferies and Davis (1993) represents the various zones of these charts. A recently updated definition of I_c by Jefferies and Been (2006) can be used to give the soil type:

$$I_c = [\{3 - \log(Q \cdot (1 - B_q) + 1)\}^2 + \{1.5 + 1.3 \cdot \log(F)\}^2]^{0.5} \tag{1}$$

where Q is the normalized tip parameter $= (q_t - \sigma_{vo})/\sigma_{vo}'$, B_q is the normalized porewater pressure parameter $= (u_2 - u_o)/(q_t - \sigma_{vo})$, F is the normalized sleeve friction $= f_s \cdot 100/(q_t - \sigma_{vo})$, σ_{vo}' is the effective overburden stress, which is the difference between total overburden stress and the hydrostatic porewater pressure $(\sigma_{vo} - u_o)$. The ranges of I_c values for different soil types can be found in the references cited above. Generally for sands, I_c is less than 2, while for clays, I_c is greater than 3.

Soil Engineering Parameters

A listing of the geotechnical parameters used in the analysis of pile foundations and the selected relationships for calculating these parameters using the CPT results are summarized in Table 1. These include the following: soil unit weight (γ_t), small-strain shear modulus (G_{max}), Young's modulus (E_{max}), preconsolidation stress (σ_p'), overconsolidation ratio (OCR), lateral stress coefficient ($K_o = \sigma_{ho}'/\sigma_{vo}'$), relative density ($D_R$) and effective stress friction angle (φ').

Table 1. Summary of selected relationships used for evaluating soil engineering parameters from SCPTu.

Relationship	Reference
Unit weight	
* $\gamma_t = 1.95 \cdot \gamma_w \cdot (\sigma_{vo}' / \sigma_{atm})^{0.06} (f_s / \sigma_{atm})^{0.06}$ — for all soil types (2)	Mayne et al. (2010)
$\gamma_t \ (kN/m^3) = 11.46 + 0.33 \cdot \log[z \ (m)] + 3.1 \cdot \log[f_s \ (kPa)] + 0.7 \cdot \log[q_t \ (kPa)]$ — for all soil types (3)	Mayne et al. (2010)
$\gamma_t \ (kN/m^3) = 8.32\log[V_s \ (m/s)] + 1.61\log[z \ (m)]$ — for all soil types (4)	Mayne (2007)
Effective stress strength	
** $\varphi' \ (degrees) = 17.6^o + 11.0 \cdot \log(q_{t1})$ — for sands (5)	Kulhawy and Mayne (1990)
* where $q_{t1} = (q_t / \sigma_{atm}) / (\sigma_{vo}' / \sigma_{atm})^{0.5}$	
*** $\varphi' \ (degrees) = 29.5^o \cdot B_q^{0.121} [0.256 + 0.336 \cdot B_q + \log Q]$ — for clays (6)	Senneset et al. (1989)
Shear wave velocity	
$V_s \ (m/s) = \{10.1 \cdot \log [q_t \ (kPa)] - 11.4\}^{1.67} \cdot [f_s \ (kPa) / q_t \ (kPa) \ 100]^{0.3}$ — for all soil types (7)	Hegazy and Mayne (1995)
$V_s \ (m/s) = 118.8 \cdot \log (f_s) + 18.5$ — for all soil types (8)	Mayne (2006)
Soil stiffness (modulus)	
$G_{max} = \rho_t \cdot V_s^2$ (9)	Timoshenko and Goodier (1951)
where, $\rho_t = \gamma_t / g_a$; and g_a is the gravitational acceleration constant $= 9.8 \ m/s^2$	
$E_{max} = 2 \cdot G_{max} \cdot (1 + \nu)$ (10)	Lehane and Cosgrove (2000)
**** Drained Poisson's ratio (ν_d) = 0.2	
Undrained Poisson's ratio (ν_u) = 0.5	
Stress history	
$\sigma_p' = 0.33 \cdot (q_t - \sigma_{vo})^m \ (\sigma_{atm} /100)^{1-m}$ — for all soil types (11)	Mayne et al. (2009) Mayne et al. (2010)
where $m = 0.65 + 1 / (800 \cdot 10^{-Ic} + 2.5)$ (12)	
* $\sigma_p' = 0.101 \cdot \sigma_{atm}^{0.102} \cdot G_{max}^{0.478} \cdot \sigma_{vo}'^{0.420}$ — for all soil types (13)	Mayne (2007)
$OCR = \{[0.192 \cdot (q_t / \sigma_{atm})^{0.22}]/[(1 - \sin\varphi') \cdot (\sigma_{vo}' / \sigma_{atm})]\}^{\{1/(\sin\varphi' - 0.27)\}}$ — for sands (14)	Mayne (2005)
Geostatic lateral stress coefficient	
$K_o = (1 - \sin\varphi') \cdot OCR^{\sin\varphi'}$ (15)	Kulhawy and Mayne (1990)
where $OCR = \sigma_p' / \sigma_{vo}'$	
Relative Density	
$D_R = 100 \cdot \{q_{t1} / (300 \cdot OCR^{0.2})\}^{0.5}$ — for sands (16)	Kulhawy and Mayne (1990)
$D_R = 100 \cdot \{0.268 \cdot \ln(q_{t1}) - 0.675\}$ — for sands (17)	Jamiolkowski et al. (2001)

* σ_{atm} is a reference stress = 100 kPa.

** For $B_q < 0.1$ corresponding to granular soils.

*** For fine-grained silts and clays, where: $0.1 < B_q < 1.0$ and $20^o < \varphi' < 45^o$.

**** ν_d values at working loads increase to larger values at failure state.

Note that G_{max} represents the true elastic region of soil behavior and therefore, a reduction factor must be applied to G_{max} for situations involving higher strains and increased levels of loading. As such, Fahey and Carter (1993) proposed the following equation:

$$G/G_{max} = 1 - f\,(\tau / \tau_{max})^g \tag{18}$$

where $\tau / \tau_{max} \approx Q / Q_{ult}$ is the mobilized load level $= 1 / FS$ (i.e., the reciprocal of factor of safety), and f and g are empirical curve fitting exponents from experimental data. Here, τ_{max} represents the shear strength of the soil, τ represents the applied shear stress, while Q_{ult} and Q represent the corresponding ultimate axial pile capacity and the operational load at any stage in loading from the minimum up to the ultimate value, respectively. Appropriate range of values for f and g are 0.98 to 1.0 and 0.3 ± 0.1, respectively, for uncemented, insensitive, and nonstructured soils of common mineralogies (i.e., kaolin, quartz, feldspar) and usual geologic origins (Mayne 2007).

Rational (Indirect) Capacity Evaluation Methods

Pile end bearing resistance (q_b) can be obtained based on limit plasticity theory whereas pile side resistance (f_p) can be found from the well-known β method that accounts for the pile material type, interface friction between soil and pile material (δ), pile installation method and σ_{vo}'. The pertinent relationships for calculating q_b and f_p are summarized in Table 2. The authors term this approach of using the entire procedure of pile capacity prediction as the rational (or indirect) method. The total axial compression capacity ($Q_t = Q_{ult}$) of a circular pile foundation is calculated from:

$$Q_t = Q_s + Q_b = \; \Sigma(f_{pi} \cdot \pi \cdot d \cdot \Delta z_i) \quad + \quad q_b \cdot \pi \cdot d^2 / 4 \tag{19}$$

where f_{pi} is the unit side resistance at i^{th} soil layer, $\pi \cdot d \cdot \Delta z_i$ is the shaft area of the ith soil layer, and Δz_i is the thickness of the ith layer. It is pertinent to mention that q_b here represents the unit base capacity of fully plugged end for open-ended pipe piles.

Table 2. Pile unit side resistance and end bearing for sands (Indirect Methods).

Relationship	Reference
* Pile unit side resistance (f_p) $f_p = C_M \cdot C_K \cdot K_o \cdot \sigma_{vo}' \cdot \tan\varphi'$ (20) where $C_M = \tan\delta/\tan\varphi'$ and $C_K = K/K_o$ are modifiers for soil-pile interaction and installation effects, respectively. Here, K is the acting lateral stress coefficient $= \sigma_h'/\sigma_v'$ and K_o is the in-situ geostatic stress coefficient $= \sigma_{ho}'/\sigma_{vo}'$. Appropriate values of C_M and C_K can be found in the reference.	Kulhawy et al. (1983)
Pile unit end bearing (q_b) ** Drained: $q_b = 0.1 \cdot {}^*N_q \cdot \sigma_{vo}'$ (21) where $^*N_q$ the bearing factor is a function of φ', appropriate values for which are presented by Vesic′ (1977).	Ghionna et al. (1994) Lee et al. (2003)

*   Generalized β-method (effective stress approach) for different soil and pile types, installation methods.
** Operational value of q_b at working load is appreciably reduced for the tolerable displacements.

Table 3. Direct CPT methods for capacity evaluation.

Method	Reference
LCPC $f_p = q_c / \alpha$ (22) $q_b = k_c \cdot q_c$ (23) where α and penetrometer bearing factor k_c depend upon the pile and soil types and the q_c, the appropriate values can be found in the reference.	Bustamante and Gianeselli 1982
* Unicone $f_p = C_{se} \cdot q_E$ (24) $q_b = C_{te} \cdot (q_t - u_2)$ (25) where the terms C_{se} and C_{te} are the side and the toe correlation coefficients	Eslami and Fellenius 1997 Fellenius 2002
** KTRI It estimates f_p from the measured f_s and the excess porewater pressure, $\Delta u_2 = u_2 - u_o$. It does not indicate a means for evaluating q_b.	Takesue et al. 1998

* See Figure 3a for soil classification and C_{se}. C_{te} is generally taken as 1. For pile diameter d > 0.4 m, $C_{te} = 1/(3d)$.
**Refer to Figure 3b for relevant expressions.

Direct Capacity Evaluation Methods

There are several direct CPT design methods used in practice that scale the data from penetrometer readings up to the axial pile resistances of driven pipe piles in sands. These include the LCPC method for all pile types (Bustamante and Gianeselli, 1982), KTRI method for driven and drilled piles (Takesue et al., 1998), and UNICONE method for driven and bored piles (Eslami and Fellenius, 1997; Fellenius 2002). Besides these, several new methods for offshore driven piles have also been derived to scale the data from cone penetration tests up to f_p and q_b. These include the FUGRO-04 method (Fugro 2004), Imperial College Pile (ICP-05) method (Jardine et al. 2005), Norwegian Geotechnical Institute (NGI-05) method (Clausen et al. 2005), and University of Western Australia (UWA-05) method (Lehane et al. 2005b). A review of these new methods can be found in Schneider et al. (2008). The methods used in this study were selected based on the experience of authors for their successful application in similar case studies and their extensive recent use in engineering practice of deep foundations. These methods are summarized in Table 3. The new offshore methods have not been considered here owing to the fact that most of these were either developed from the database which already included the EURIPIDES project or these methods have already been applied at this site (e.g., Clausen et al. 2005, Fugro 2004, Jardine et al. 2005, Kolk et al. 2005, Lehane et al. 2005a, b, Schneider and Lehane 2005, Schneider et al. 2008).

A representation of the KTRI and Unicone methods in chart forms is shown in Figure 3. For the LCPC method, it is relevant to mention that the maximum appropriate value of penetrometer bearing capacity factor, k_c, should be adopted for the closed ended pipe pile or if, full-scale loading test indicates that the plug is capable of taking up the load equivalent of a closed ended pile of the same diameter.

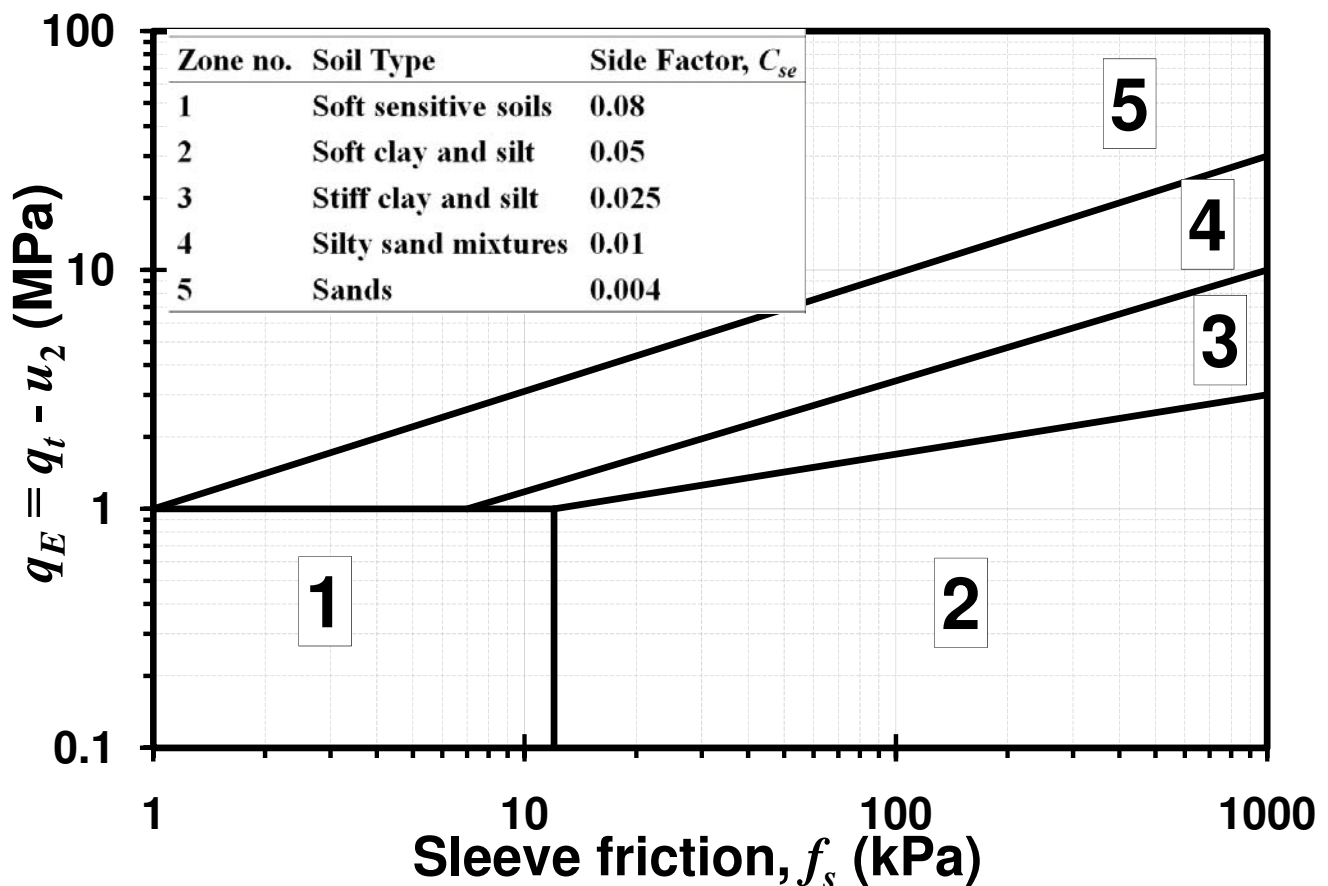| Zone no.	Soil Type	Side Factor, C_{se}
1	Soft sensitive soils	0.08
2	Soft clay and silt	0.05
3	Stiff clay and silt	0.025
4	Silty sand mixtures	0.01
5	Sands	0.004

Figure 3. (a) Unicone chart for zone number and soil type (after Eslami and Fellenius 1997).
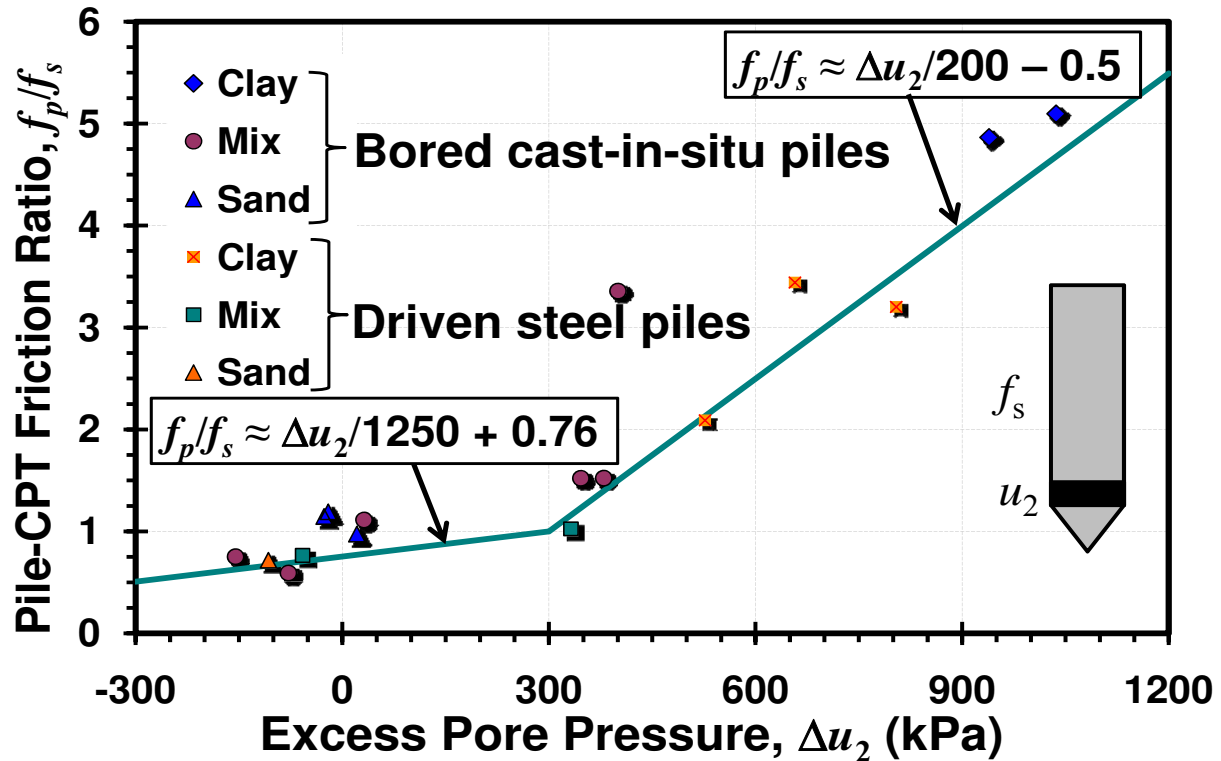
Figure 3. (b) KTRI method for side friction of piles (after Takesue et al. 1998).

ELASTIC CONTINUUM SOLUTION

The pile response in terms of load-displacement and axial load transfer along the pile shaft (Q_s) and to the pile base (Q_b) can be evaluated from the analytical closed-form elastic continuum pile solution given by Fleming et al. (1992), and Randolph (2003). The solution is summarized in Figure 4 and accounts for piles in homogeneous soils (having constant G with depth) as well as the Gibson-type soil models (having a linearly-varying G with depth). It also encompasses the floating-type pile ($G_{sL} = G_{sb}$) or the end-bearing type where the pile base rests on a stiffer stratum ($G_{sb} > G_{sL}$). Figure 4 also shows a model proposed for layered soils in which the capacity of each segment of the pile embedded in i[th] layer can be evaluated. Accordingly, the load-displacement response for each segment of the pile embedded in i[th] layer corresponding to the load transferred through that layer can be conveniently obtained and integrated to find the overall response of the pile.

EURIPIDES PILE RESPONSE EVALUATION

In order to use the applicable SCPTu-based pile response evaluation methods, data from sounding SCPTu-36 were utilized for the input parameters and analysis. The measured u_1 readings shown in Figure 2 were converted to u_2 via the relationships: $u_2 = 0.742 \cdot u_1$ (Chen and Mayne 1994) for clay and silt layers, while for sand layers u_2 was taken to be equal to u_1 (Bruzzi and Battaglio 1987). Since the soil profile at the site consists essentially of sand, the overall effect of the conversion of u_1 to u_2 is minimal. The measured cone tip resistance (q_c) values were also taken as comparable to the total cone tip resistance (q_t), since the correction is not considered significant for sands and dense granular soils (Mayne 2007). From the compression/tension loading sequence, only the first set of compression tests was analyzed for each of the three test depths.

Soil Classification and Soil Engineering Parameters Evaluation from SCPTu-36 Data

The first step in the analysis was evaluation of soil engineering parameters at the site using appropriate correlations shown in Table 1. Figure 5 presents the soil classification and engineering parameters so obtained by the post processing of data from SCPTu-36. To validate the applicability of SCPTu based correlations, the measured values of unit weight (γ_t) and shear wave velocity (V_s) from the site (Fugro 2004) were also plotted. For the most part, the values obtained from averaging the correlations' results tend to match well with the measured values.
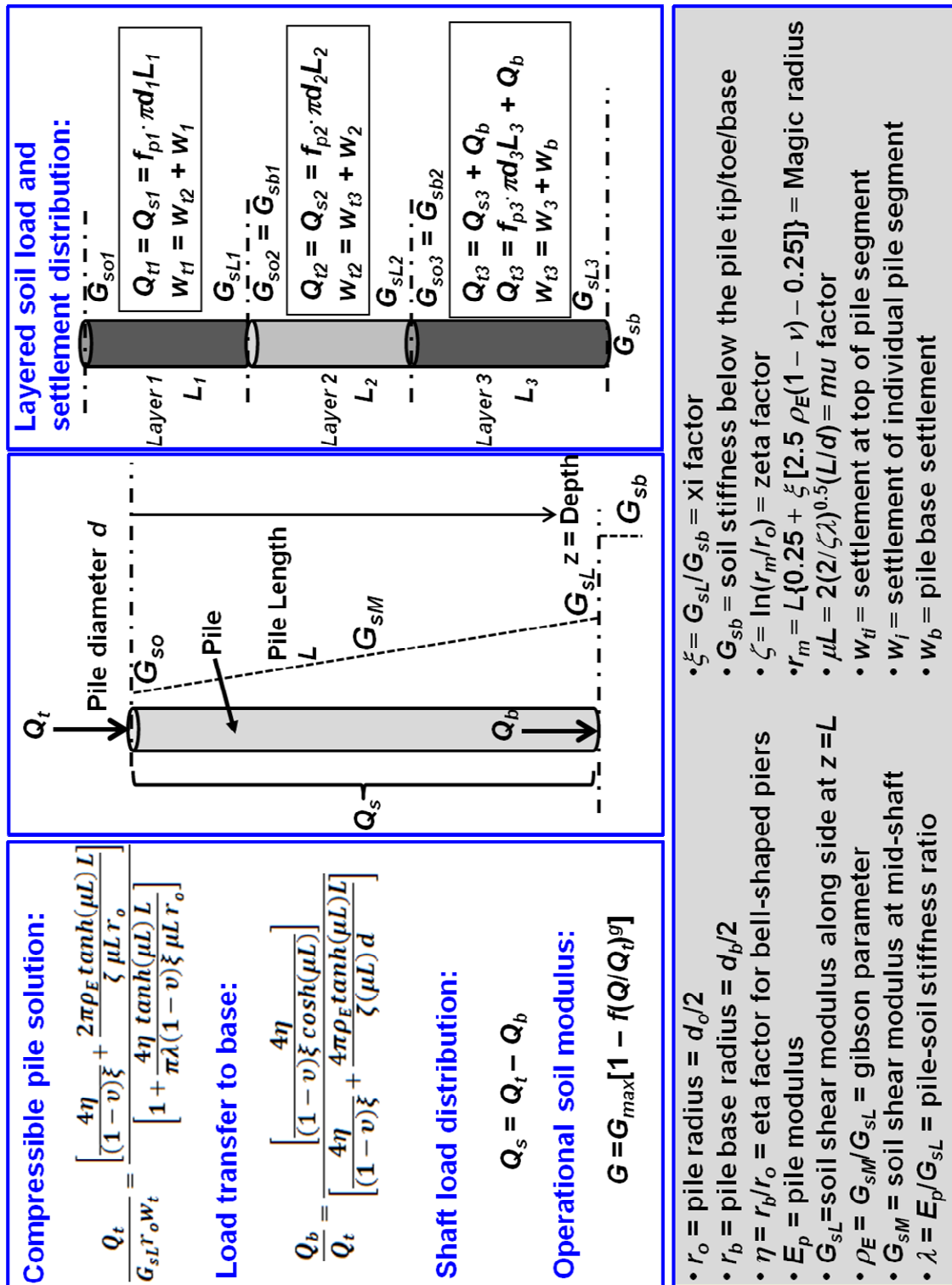
Layered soil load and settlement distribution:

$\bar{G}_{so1}$

Layer 1, L_1

$Q_{t1} = Q_{s1} = f_{p1} \cdot \pi d_1 L_1$
$w_{t1} = w_{t2} + w_1$

G_{sL1}
$\bar{G}_{so2} = \bar{G}_{sb1}$

Layer 2, L_2

$Q_{t2} = Q_{s2} = f_{p2} \cdot \pi d_2 L_2$
$w_{t2} = w_{t3} + w_2$

G_{sL2}
$\bar{G}_{so3} = \bar{G}_{sb2}$

Layer 3, L_3

$Q_{t3} = Q_{s3} + Q_b$
$Q_{t3} = f_{p3} \cdot \pi d_3 L_3 + Q_b$
$w_{t3} = w_3 + w_b$

G_{sL3}
G_{sb}

Pile diameter d · Pile · Pile Length L · Q_t · Q_b · Q_s · $\bar{G}_{so}$ · G_{sM} · G_{sL} · G_{sb} · z = Depth

---

Compressible pile solution:

$$\frac{Q_t}{G_{sL}r_o w_t} = \frac{\left[\dfrac{4\eta}{(1-v)\xi} + \dfrac{2\pi\rho_E\,tanh(\mu L)\,L}{\zeta\,\mu L\,r_o}\right]}{\left[1 + \dfrac{4\eta}{\pi\lambda(1-v)\,\xi}\dfrac{tanh(\mu L)\,L}{\mu L\,r_o}\right]}$$

Load transfer to base:

$$\frac{Q_b}{Q_t} = \frac{\left[\dfrac{4\eta}{(1-v)\,\xi}\dfrac{1}{cosh(\mu L)}\right]}{\left[\dfrac{4\eta}{(1-v)\,\xi} + \dfrac{4\pi\rho_E\,tanh(\mu L)\,L}{\zeta(\mu L)\,d}\right]}$$

Shaft load distribution:

$Q_s = Q_t - Q_b$

Operational soil modulus:

$G = G_{max}[1 - f(Q/Q_t)^g]$

- r_o = pile radius = $d_o/2$
- r_b = pile base radius = $d_b/2$
- $\eta = r_b/r_o$ = eta factor for bell-shaped piers
- E_p = pile modulus
- G_{sL} = soil shear modulus along side at z =L
- $\rho_E = G_{sM}/G_{sL}$ = gibson parameter
- G_{sM} = soil shear modulus at mid-shaft
- $\lambda = E_p/G_{sL}$ = pile-soil stiffness ratio
- $\xi = G_{sL}/G_{sb}$ = xi factor
- G_{sb} = soil stiffness below the pile tip/toe/base
- $\zeta = \ln(r_m/r_o)$ = zeta factor
- $r_m = L\{0.25 + \xi[2.5\ \rho_E(1 - v) - 0.25]\}$ = Magic radius
- $\mu L = 2(2/\zeta\lambda)^{0.5}(L/d)$ = mu factor
- w_{ti} = settlement at top of pile segment
- w_i = settlement of individual pile segment
- w_b = pile base settlement

Figure 4. Elastic pile solution for load-displacement response of pile foundations.
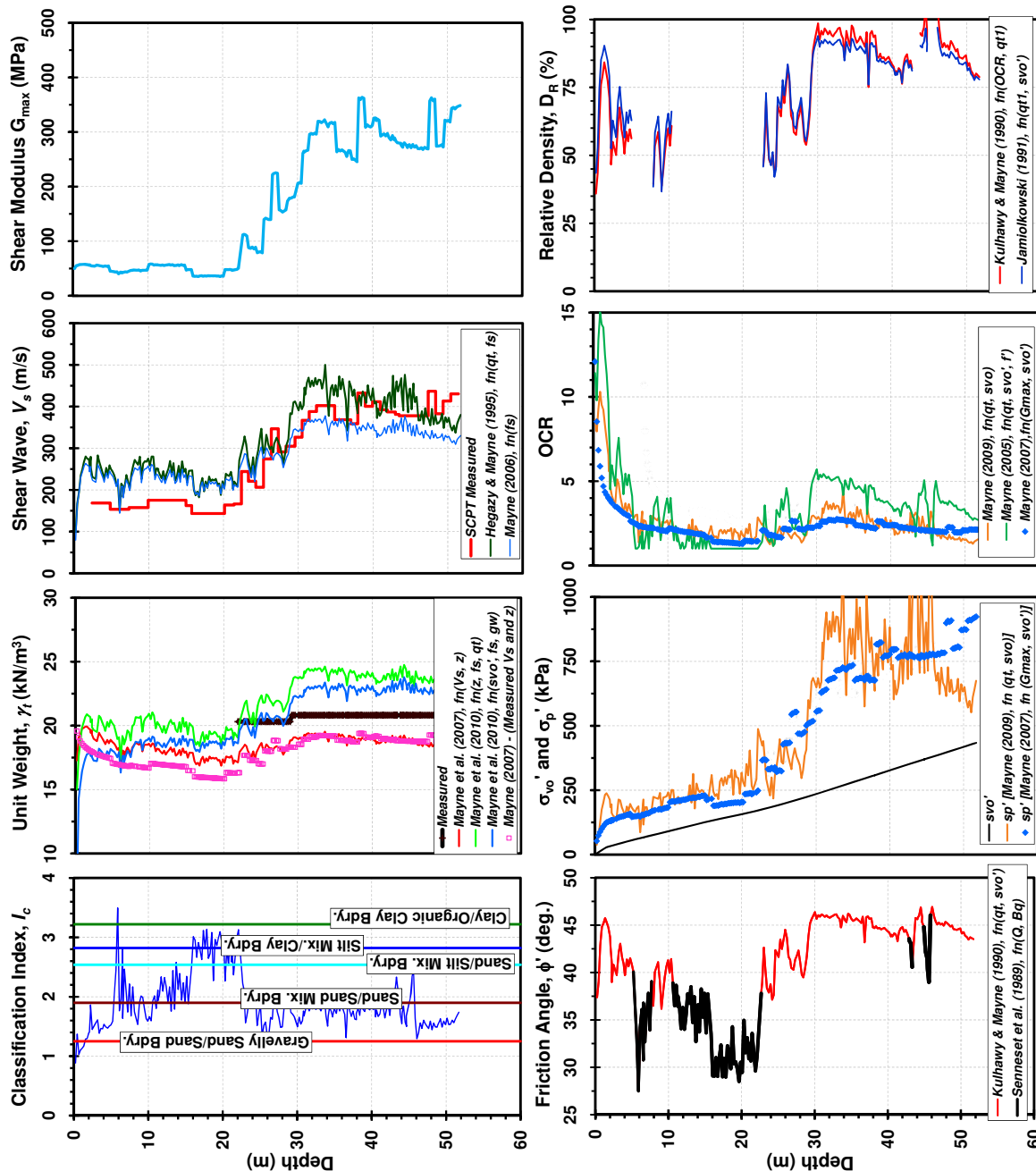
Figure 5. Profiles of soil engineering parameters at EURIPIDES test site (location 1) from SCPTu-36 data.

Evaluation of pile capacities from CPT methods

Subsequent to validation of the soil classification and the evaluation of soil engineering parameters, pile side and base capacities were calculated for three penetration depths (30.5 m, 38.7 m, and 47.0 m) using the CPT methods described previously. For each test, the soil strata at the site were divided into multiple layers, keeping in view the soil profiles (see Figures 2 and 5) and the relevant pile embedment depth. The mean value of G_{max} was calculated for each layer as shown in Figure 6. Applicable layers considered for the three pile load tests were as follows: (1) for 30.5 m pile embedment – layers 1 through 6; (2) for 38.7 m pile embedment – layers 1 through 8; and (3) for 47.0 m pile embedment – layers 1 through 11. The total pile side capacity (Q_s) for each test depth was calculated from the summation of individual side capacities of applicable layers (i.e. ΣQ_{si}), which in turn were found from the product of mean unit side resistance of the layer (f_{pi}) and surface area of the respective pile segment in that layer ($\pi \cdot d_i \cdot l_i$).
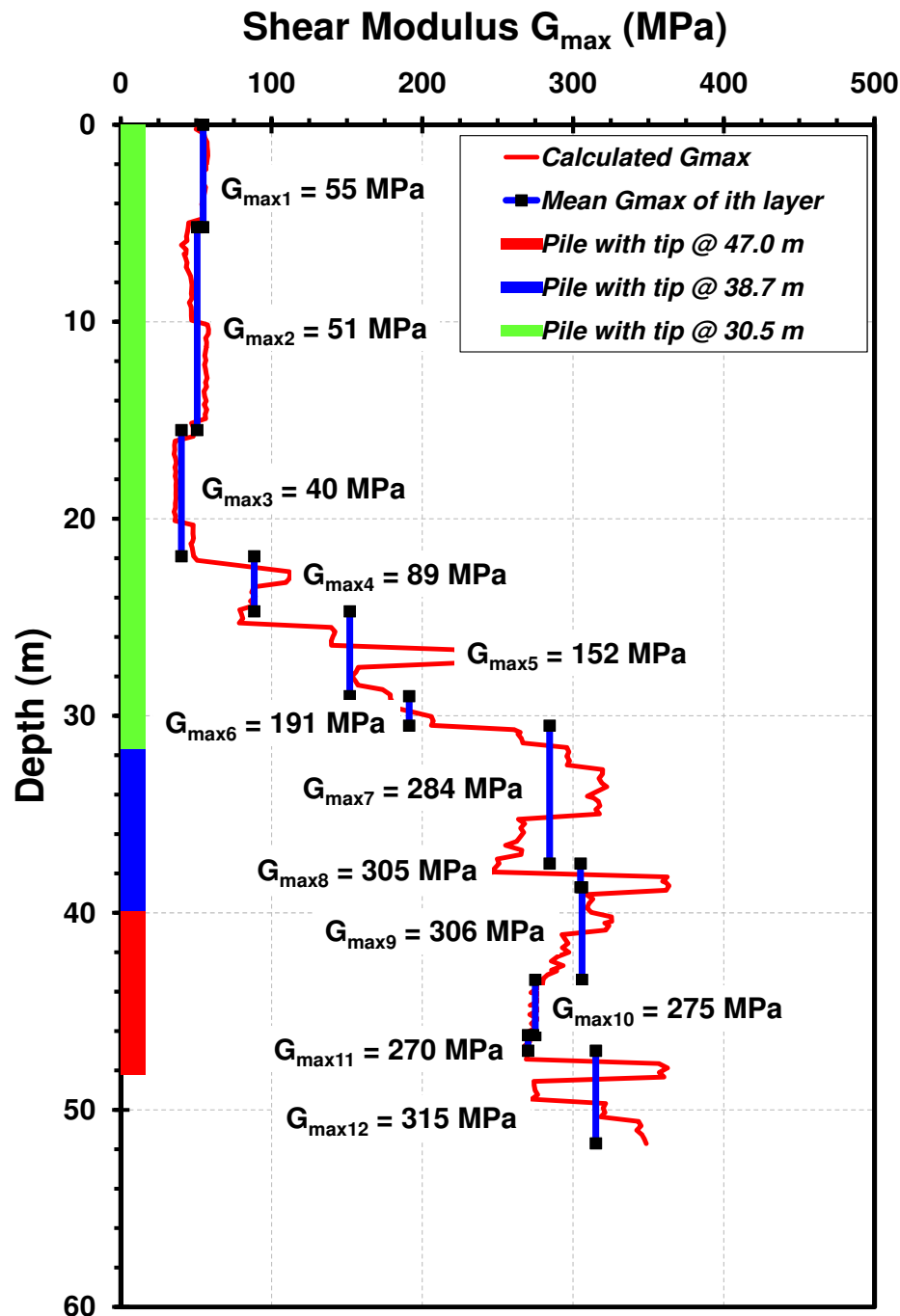
Figure 6. Profile of Small Strain Shear Modulus, G_{max} for soil layers at EURIPIDES test site.

The authors considered it appropriate to use different CPT methods to observe how well they compare with each other and with the measured results. Accordingly, selected methods described earlier were applied to evaluate f_p values for the relevant layers and q_b values for three pile embedment depths. A summary of the f_p values obtained is given in Table 4. The total pile side capacities (Q_s) and base capacities (Q_b), and the total pile capacities (Q_t) for the three test depths derived from multiple CPT methods as compared to the measured results are shown in a summarized form in Tables 5 and 6. Analysis of the results from this case study leads to the following findings/deductions concerning the selected CPT methods:

- LCPC method yielded the lowest values of f_p for all test depths, whereas, the opposite is true for q_b. Inherent in this method is the limiting condition for f_p, which restricts the result to certain maximum values for all natures of soils

and all pile production and placement methods. For calculating q_b using the LCPC method, maximum relevant value of $k_c = 0.4$ was adopted, as it was known from Fugro (2004) that a 0.65-m thick strong disk of wood got wedged into the pile toe plug area presumably at around 22 m depth bgl (significantly above the pile embedment depths for all the three load tests). Based on this information, the pile was assumed to be capable of taking up the loads equivalent of a closed ended or fully plugged pile for the load tests at all three embedment depths.

- β-method also predicted low values of f_p, only slightly higher than those found from LCPC method. It is observed that the values specified for the soil-pile interaction modifier term C_M in this method accounts for the pile roughness without consideration to the soil type. With the same type of pile, interface friction in medium to dense sand is reasonably expected to be much higher than that in soft clays.

- KTRI method, which estimated only the f_p resistance, yielded much higher values of this parameter compared to all other methods considered for all three test depths. This observation is more relevant to the layers beneath 22m depth, where the sand was found to be much denser than the upper layers. The authors have observed by conducting similar case studies that the KTRI method generally overestimates f_p values in very dense sands, and the current study substantiates this observation.

- The limit plasticity solution used to evaluate q_b compared most favorably to the values obtained from load tests. These values were found to be slightly less than the measured values. As seen from equation (21) in Table 2, the values of q_b were substantially reduced (one-tenth of the total value). This was done to account for the tolerable displacements and strain incompatibility differences occurring between unmatched mobilization of side resistance and end-bearing components in sands, as recommended by Ghionna et al. (1994). This factor might be attributed as the cause for the slight underestimation of operational q_b as higher mobilization of end bearing could have possibly occurred compared to the assumption.

- Of all the selected methods, f_p values found from UNICONE method matched most closely to the measured results. In contrast this method gives the lowest values of q_b, compared to the other selected methods. Specified in this method, the toe correlation coefficient C_{te} for calculating q_b accounts for pile diameter only without consideration to soil or pile type.

- The estimates of Q_t from LCPC method apparently compared well to the measured values (see Table 6). However, as discussed earlier, the same is not true for the separate components of Q_b and Q_s estimated from LCPC method. Thus, comparisons of the separate components of pile capacities (Q_b and Q_s) to the measured results are considered more logical.

The authors found that an averaging of q_b and f_p from these methods resulted in total capacities that compared more favorably to the measured capacities than the capacities obtained using any individual method. Whether this averaging technique would work well in other situations needs to be investigated.

Because of the fact that none of the methods alone yielded reasonably comparable values of the two components of pile capacities together with the measured ones, the authors had to backfigure the capacities in order to use the most appropriate ones to be applied in the elastic continuum solution and predict the load-displacement response for each test depth. An alternate approach was adopted by applying the hyperbolic fitting model proposed by Kondner (1963) to the measured load-displacement for the pile tests conducted at three penetration depths. This model gives the transformed hyperbolic representation of load-displacement to find Q_{ult} as inverse of the transformed slopes. The results thus found were also comparable to the average values (see Figure 7). Accordingly, these values were selected to plot the evaluated load-displacement response from the elastic continuum solution.

The f_p profiles and the pile load distributions for the three penetration depths obtained from the above described methods are shown in graphical form in Figure 8. The discrepancies between the adopted CPT-based estimates and the measured values of side resistance observed near the pile tip can possibly be attributed to the fact reported by Fugro (2004) that the measured values shown are the average outer friction and that there is likelihood of significant friction between the soil plug and the inner pile wall near the pile tip during compression loading. Hence, the average unit friction on the inner and the outer wall of the pile near the pile toe may be in-between the presented measured values and half these values. Other factors contributing to these discrepancies could be that the measured axial forces at the pile tip were computed from the strain gauges 0.38m above the pile tip because, as previously mentioned, the toe load cell was damaged during pile driving.
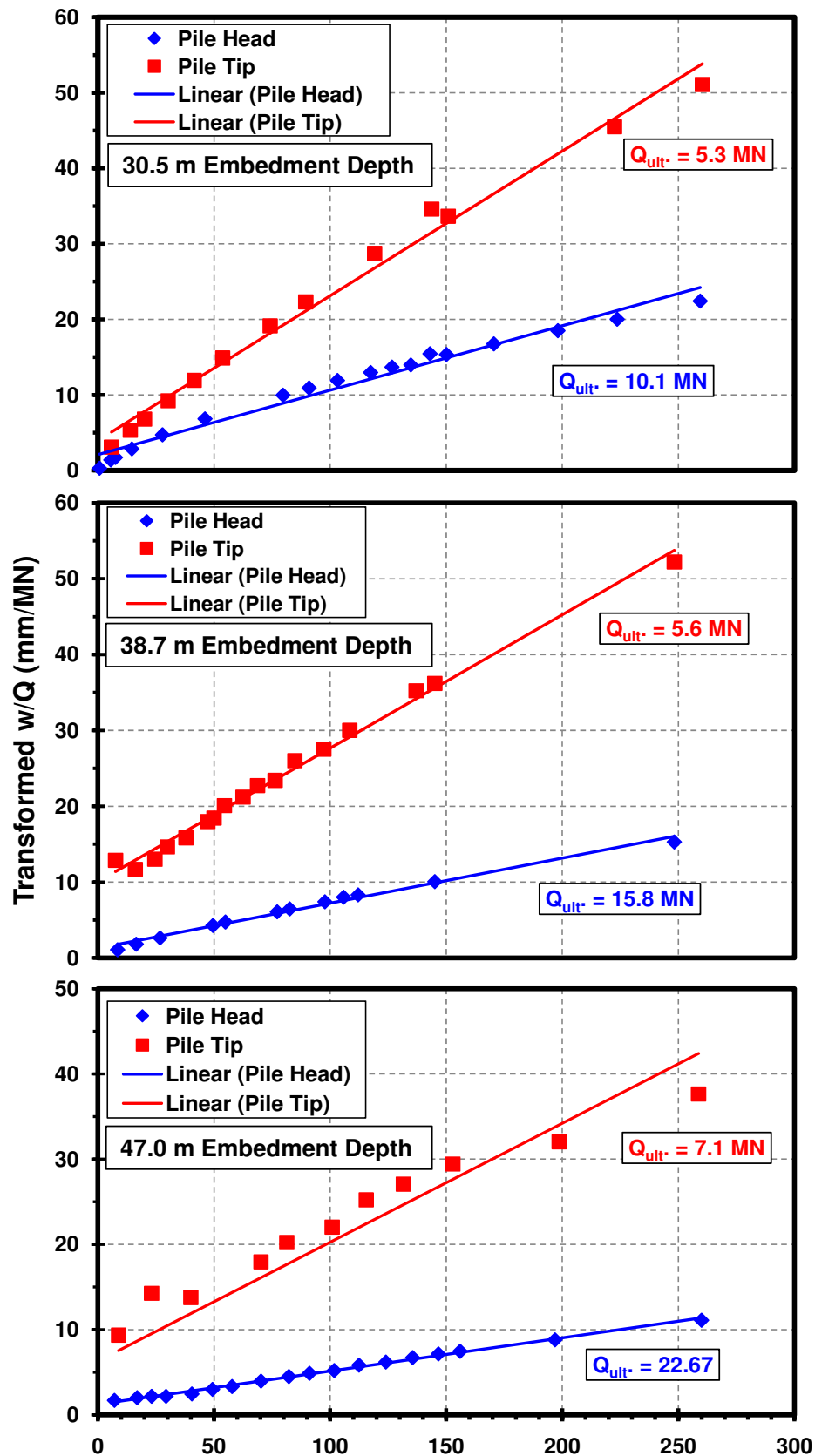
Figure 7. Q_{ult} from measured load-displacement results of the EURIPIDES pile load tests from hyperbolic fitting model by Kondner (1963).
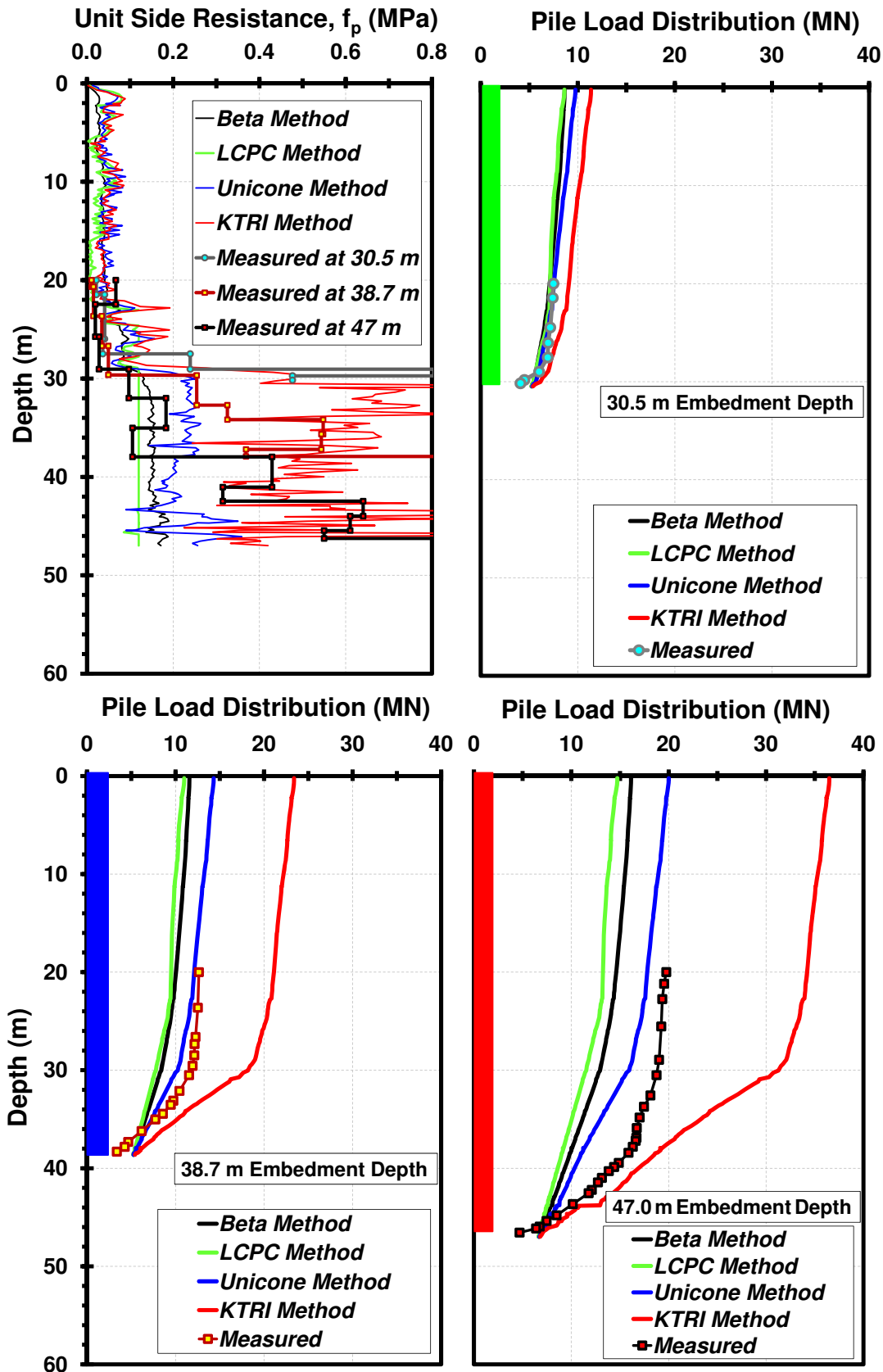
Figure 8. Unit side resistance and pile load distributions at 30.5 m, 38.7 m and 47.0 m embedment depths.

Table 4. Pile side capacities for layered soil from different CPT methods.

i^{th} Soil Layer	Mean unit side resistance for i^{th} soil layer, f_{pi} (kPa)					*Shaft capacity of ith layer, Q_{si} (MN)
	LCPC	Unicone	KTRI	Beta	Mean	
Layer 1 (0-5.2 m)	49.4	45.8	54.0	24.2	43.4	0.54
Layer 2 (5.2-15.5 m)	30.2	48.9	49.4	33.0	40.4	0.99
Layer 3 (15.5-21.9 m)	11.8	41.2	37.5	40.6	32.8	0.51
Layer 4 (21.9 - 24.7 m)	56.7	62.9	85.9	59.8	66.3	0.45
Layer 5 (24.7-29 m)	106.7	94.8	140.2	83.5	106.3	1.09
Layer 6 (29-30.5 m)	119.6	193.3	405.0	120.6	209.6	0.76
Layer 7 (30.5-37.5 m)	120.0	234.2	626.9	148.4	282.4	4.74
Layer 8 (37.5-38.7 m)	120.0	216.8	494.8	150.6	245.6	0.71
Layer 9 (38.7-43.4 m)	119.9	182.9	479.6	151.2	233.4	2.63
Layer 10 (43.4-46.2 m)	117.4	237.5	625.8	167.9	287.2	1.93
Layer 11 (46.2-47.0 m)	120.0	268.7	369.8	171.3	232.4	0.45

* $Q_{si} = f_{pi} \cdot \pi \cdot d_i \cdot l_i$

Table 5. Pile base and shaft capacities from different CPT methods.

Test pile embedment depth (m)	Base Capacity, Q_b (MN)					* Total Shaft Capacity, Q_s (MN)					
	LCPC	Unicone	Limit Plasticity	Mean	** Measured	LCPC	Unicone	KTRI	Beta	Mean	** Measured
30.5	10.6	1.2	3.7	5.2	4.6	3.4	4.6	6.1	3.5	4.4	6.0
38.7	9. 7	1.1	4.8	5.2	4.9	5.8	9.1	18.2	6.4	9.9	10.6
47.0	12.5	1.3	5.9	6.6	6.5	8.2	13.4	29.9	9.5	15.3	16.2

* $Q_s = \Sigma f_{pi} \cdot \pi \cdot d_i \cdot l_i$

** after Fugro 2004.

Table 6. Total pile capacities from different CPT methods.

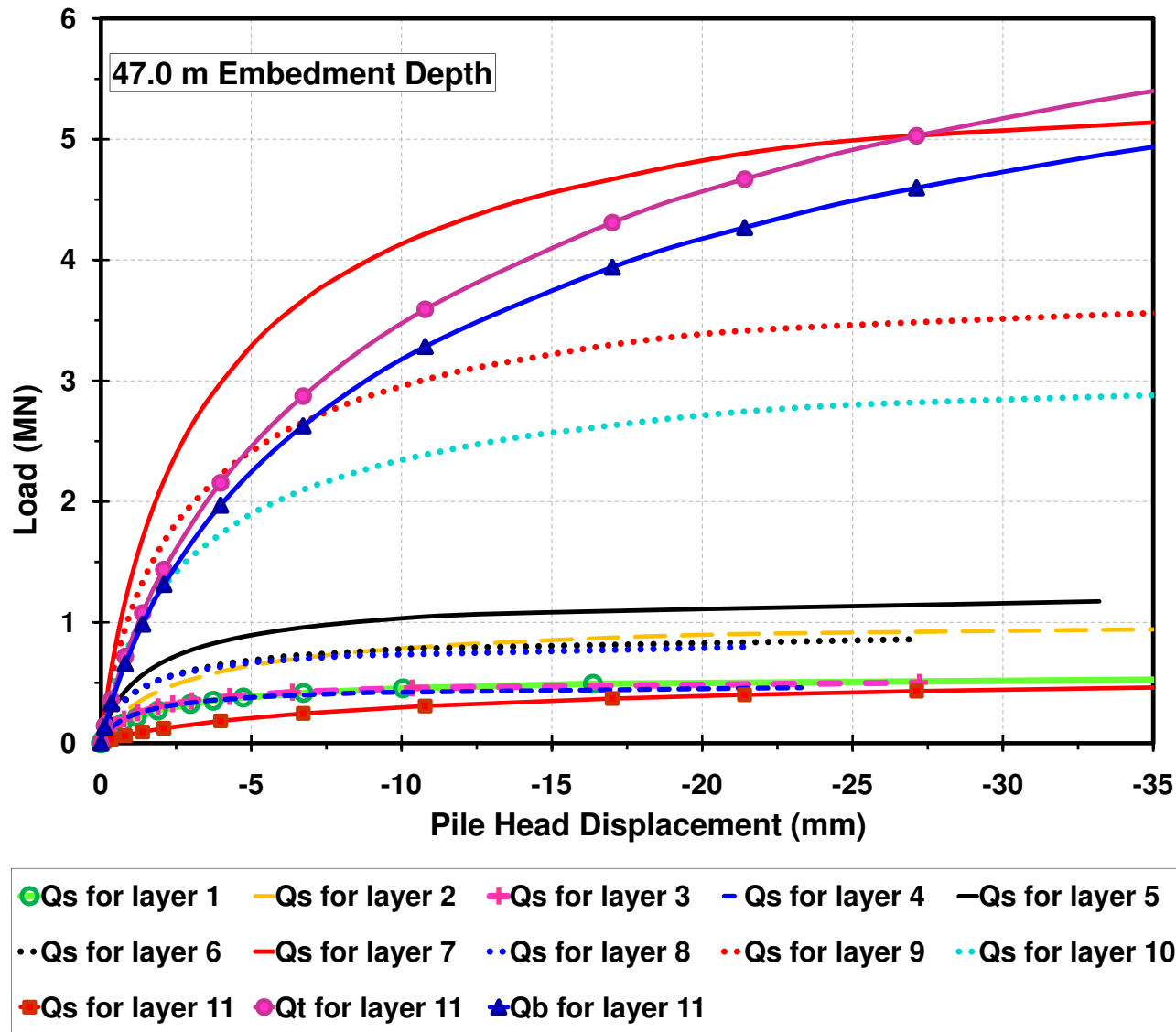| Test pile embedment depth (m)	Total Capacity, Q_t (MN)				
	LCPC	Unicone	Rational	* Mean	** Measured
30.5	14.0	5.8	7.2	9.6	10.6
38.7	15.5	10.2	11.2	15.1	15.5
47.0	20.7	14.7	15.4	21.9	22.7

* Mean evaluated Q_t values were obtained by including Q_s values from KTRI method also.

** after Fugro 2004.

Load-displacement evaluation

In order to evaluate the load-displacement response from the elastic continuum solution, independent responses of each segments of the pile embedded through its corresponding layer were first evaluated using the applicable side and base capacities already calculated (mean values in Table 4 and 5) for the layers relevant to the pile test depth. The values of G_{max} from Figure 6 were used for each of the pertinent layers and the G values applicable to the operational loads were calculated using the modulus reduction scheme given in equation (18). As an example, independent load-displacement responses for eleven layers obtained for the 47.0 m of pile embedment depth are shown in Figure 9. Cumulative load-displacement curves (Q_t vs. w_t, Q_s vs. w_t and Q_b vs. w_t) for all three test depths, shown in Figure 10, were obtained by integrating the independent responses for all pertinent layers corresponding to each test depth. A reasonably good match was observed between the measured and evaluated responses for all three test depths.

Figure 9. Layered soil load-displacement distribution for EURIPIDES pile load tests.

47.0 m Embedment Depth

Load (MN)

Pile Head Displacement (mm)

Legend:
- Qs for layer 1
- Qs for layer 2
- Qs for layer 3
- Qs for layer 4
- Qs for layer 5
- Qs for layer 6
- Qs for layer 7
- Qs for layer 8
- Qs for layer 9
- Qs for layer 10
- Qs for layer 11
- Qt for layer 11
- Qb for layer 11

47.0 m Embedment Depth

Layer 1
(0 – 5.2 m)
Qt1 = Qs1 = 540.37 kN

Layer 2
(5.2 – 15.5 m)
Qt2 = Qs2 = 996.59 kN

Layer 3
(15.5 – 21.9 m)
Qt3 = Qs3 = 502.73 kN

Layer 4
(21.9 – 24.7 m)
Qt4 = Qs4 = 459.97 kN

Layer 5
(24.7 – 29.0 m)
Qt5 = Qs5 = 1173.95 kN

Layer 6
(29.0 – 30.5 m)
Qt6 = Qs6 = 860.47 kN

Layer 7
(30.5 – 37.5 m)
Qt7 = Qs7 = 5508.98 kN

Layer 8
(37.5 – 38.7 m)
Qt8 = Qs8 = 797.35 kN

Layer 9
(38.7 – 43.4 m)
Qt9 = Qs9 = 3765.89 kN

Layer 10
(43.4 – 46.2 m)
Qt10 = Qs10 = 3083.57 kN
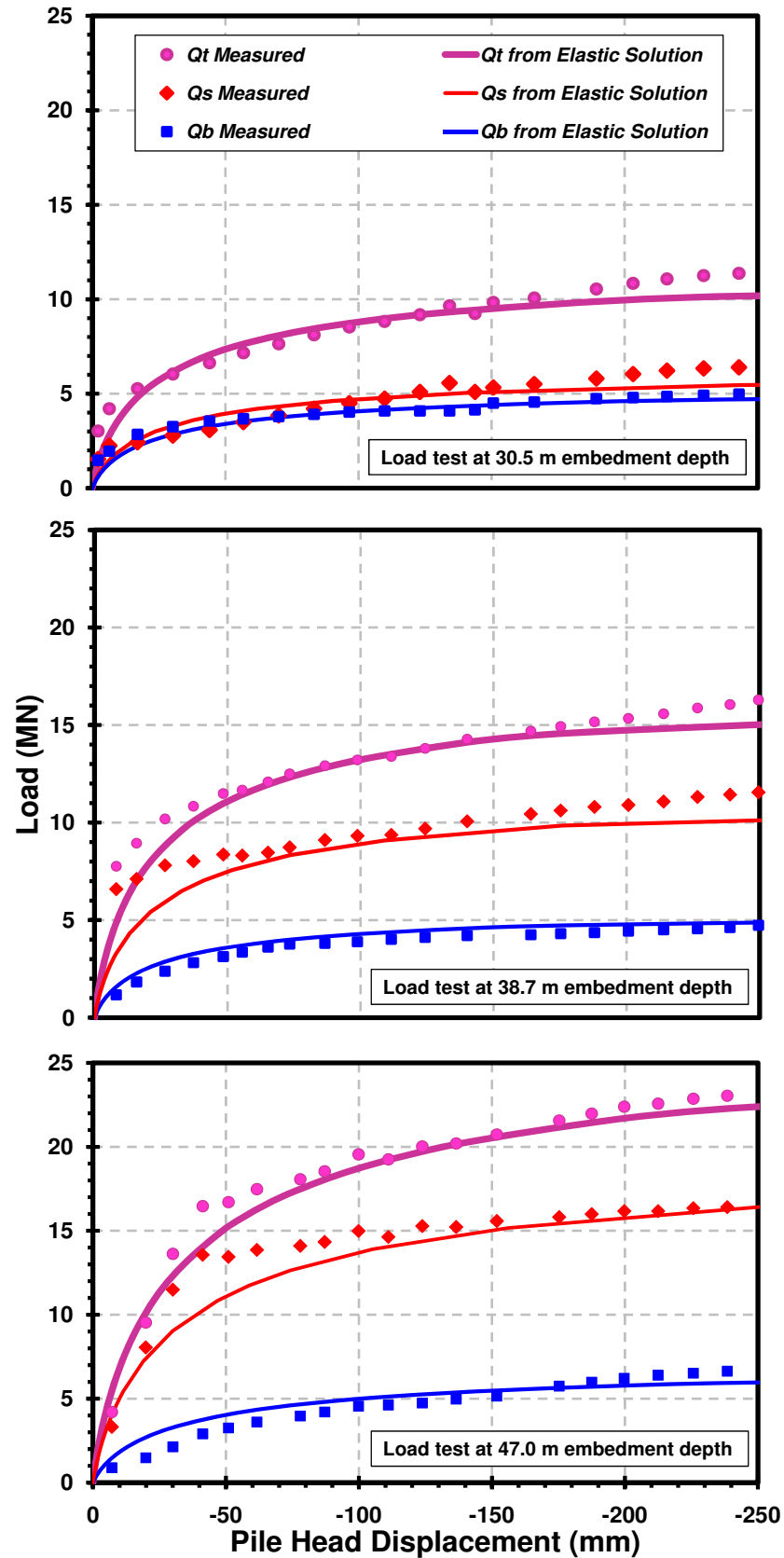
Layer 11
(46.7 – 47.0 m)
Qt11 = Qs11+Qb = 7183.99 kN

Figure 10. Load-displacement response for pile tests at location 1 EURIPIDES (measured and evaluated).

CONCLUSIONS

This case study presented a brief review of the pile load tests conducted for EURIPIDES project involving a driven open-ended pipe pile in dense sands for which soil boring and seismic piezocone penetration test (SCPTu) data are available. Three direct and two indirect CPT methods were used to estimate the ultimate axial load capacity of the pipe pile that was load tested after successive driving to three different test depths. Analyses were performed to evaluate the selected CPT methods by comparing the estimated and measured ultimate pile capacities and load-transfer through depth. The load-displacement response through the layered soil profile at the site was assessed using backfigured capacities found by averaging of multiple CPT methods in the elastic continuum solution and the G_{max} reduction scheme for increasing loads to account for the nonlinear soil response.

For this study, it was found that q_b and f_p components of the pile capacity can be determined within the range of reasonable accuracy by careful application of multiple CPT methods. The reliability of individual CPT methods cannot be afforded on the basis of just one case study. For more information on the reliability of these individual methods, readers are referred to studies and reviews reported by Cai et al. (2009), Ardalan et al. (2008), and Abu-Farsakh and Titi (2004).

From the results of this study, the following were observed concerning the performance of CPT methods:

- Unicone method proved best for estimating f_p, though the estimates were slightly less than the measured values; this method, however, substantially underestimated q_b;

- KTRI method substantially overestimated f_p, especially in very dense sand layers;

- LCPC method underestimated f_p, while it overestimated q_b appreciably;

- β-method underestimated f_p; these estimates were closest to those found from LCPC method; and

- Limit plasticity method yielded best estimates of q_b.

The predictions from Unicone, KTRI and LCPC methods for this case are consistent with the results of reliability studies by Cai et al. (2009) and Ardalan et al. (2008) concerning these methods as applied to other cases.

The backfigured capacities from multiple CPT methods applied to elastic continuum solution yielded complete load-displacement-capacity responses that were found reasonable when compared to the measured results.

In summary, for the EURIPIDES static pile load tests, the averaging of multiple CPT methods provided calculated pile capacities within reasonable agreement with the capacity determined in the tests. The data from SCPTu can be conveniently utilized to estimate the entire load-displacement-capacity response of the pile loaded axially. Consequently, the SCPTu method is simple, quick, and easy to apply in the engineering analysis of piles, but significant engineering judgment must be applied for interpretation of the results.

ACKNOWLEDGMENTS

REFERENCES

Abu-Farsakh, M.Y. and Titi, H.H. (2004). "Assessment of direct cone penetration test methods for predicting the ultimate capacity of friction driven piles." J. of Geotechnical and Geoenvironmental Engrg., ASCE, 130(9), 935 – 944.

Ardalan, H., Eslami, A. and Nariman-Zahed, N. (2009). "Piles shaft capacity from CPT and CPTu data by polynomial neural networks and genetic algorithms." Computers and Geotechnics 36, 616–625.

Bruzzi, D., and Battaglio, M. (1987). "Pore pressure measurements during cone penetration tests." Report No. 229, I quaderni dell'ISMES, Experimental Institute for Models and Structures, Milan, 125p.

Bustamante, M., and Gianeselli, L. (1982). "Pile bearing capacity predictions by means of static penetrometer CPT." Proc., 2nd European Symposium on Penetration Testing (ESOPT-II), Vol. 2, Amsterdam, 493 – 500.

Cai, G., Liu, S., Tong, L. and Du, G. (2009). "Assessment of direct CPT and CPTU methods for predicting the ultimate bearing capacity of single piles." Engineering Geology 104, 211–222.

Clausen, C.J.F., Aas, P.M., and Karlsrud, K. (2005). "Bearing capacity of driven piles in sand, the NGI approach." Frontiers in Offshore Geotechnics (Proc.ISFOG, Perth), Taylor & Francis, London, 677–681.

Chen, B.S.Y. and Mayne, P.W. (1994). "Profiling the overconsolidation ratio of clays by piezocone tests." Report GIT-CEEGEO-94-1, Civil Engineering, Georgia Institute of Technology, Atlanta, 280 p.

Eslami, A., and Fellenius, B.H. (1997). "Pile capacity by direct CPT and CPTu methods applied to 102 case histories." Canadian Geotechnical Journal, 34 (6), 880 – 898.

Fahey, M., and Carter, J.P. (1993). "A finite element study of the pressuremeter in sand using a nonlinear elastic plastic model." Canadian Geotechnical Journal, 30 (2), 348 – 362.

Fellenius, B.H. (2002). Excerpt from Chapter 6 of the Red Book: Direct methods for estimating pile capacity, in Background to UniCone <http://www.fellenius.net>. accessed May 22, 2010.

Fleming, W.G.K., Weltman, A.J., Randolph, M.F., and Elson, W.K. (1992). Piling Engineering. 2nd ed., Blackie/Halsted Press, John Wiley & Sons, NY, 122 – 128.

Fugro (2004). "Axial pile capacity design method for offshore driven piles in sand." Report to American Petroleum Institute, No. P1003, Issue 3, Houston, Texas, 122p.

Ghionna, V.N., Jamiolkowsi, M., Pedroni, S., and Salgado, R. (1994). "The tip displacement of drilled shafts in sands." Vertical and Horizontal Deformations of Foundations and Embankments, Vol. 2, GSP 40, ASCE, Reston/VA, 1039–1057.

Google Map. (2009). "Satellite image." <www.maps.google.com> accessed May 19, 2010.

Hegazy, Y.A., and Mayne, P.W. (1995). "Statistical correlations between Vs and CPT data for different soil types." Proc., International Symposium on Cone Penetration Testing, Vol. 2, Swedish Geotechnical Society, Linköping, Sweden, 173 – 178.

Holtz, W.G. (1973). "The relative density approach – uses, testing requirements, reliability, and shortcomings." Proc. Symp. Evaluation of Relative Density and Its Role in Geotechnical Projects Involving Cohesionless Soils, ASTM STP 523, Philadelphia, 5 – 17.

Jamiolkowski, M., LoPresti, D.C.F., and Manassero, M. (2001). "Evaluation of relative density and shear strength of sands from cone penetration test and flat dilatometer test." Soil Behavior and Soft Ground Construction (GSP 119), American Society of Civil Engineers, Reston, VA, 201 – 238.

Jardine, R., Chow, F., Overy, R., and Standing, J. (2005). ICP design methods for driven piles in sands and clays. Thomas Telford Publishing, London.

Jefferies, M.G., and Been, K. (2006). Soil Liquefaction – a critical state approach. Taylor and Francis Group, London, 480 p.

Jefferies, M.G., and Davies, M.P. (1991). "Soil classification by the cone penetration test: Discussion." Canadian Geotechnical J., 28 (1): 173–176.

Jefferies, M.G., and Davies, M.P. (1993). "Use of CPTu to estimate equivalent SPT N60." Geotechnical Testing J., ASTM, 16 (4): 458–468.

Kolk, H.J., Baaijens, A.E., and Vergobi, P. (2005). "Results of axial load tests on pipe piles in very dense sands: The EURIPIDES JIP." Frontiers in Offshore Geotechnics (Proc. ISFOG, Perth) Taylor & Francis, London, 661 – 667.

Kondner, R.L. (1963). "Hyperbolic stress-strain response: cohesive soils." ASCE J. of Soil Mechanics and Foundations Div. 89 (1), 115-143.

Kulhawy, F.H., and Mayne, P.W. (1990). "Manual on estimating soil properties for foundation design." Report EPRI EL-6800, Electric Power Research Institute, Palo Alto, CA, 306p.

Kulhawy, F.H., Trautmann, C.H. Beech, J.F. O'Rourke, T.D., and McGuire, W. (1983). "Transmission line structure foundations for uplift-compr. loading." Report EL-2870, Electric Power Research Institute, Palo Alto, Calif., 412p.

Lee, J., Salgado, R., and Paik, K. (2003). "Estimation of load capacity of pipe piles in sand based on CPT Results." J. of Geotechnical and Geoenvironmental Engrg., ASCE, 129(5), 391 – 403.

Lehane, B., and Cosgrove, E. (2000). "Applying triaxial compression stiffness data to settlement prediction of shallow foundations." Geotechnical Engineering, Vol. 142, 19 – 200.

Lehane, B.M., Schneider, J.A., and Xu, X. (2005a). "A review of design methods for offshore driven piles in siliceous sand." UWA Report No.GEO 05358, Univ. of Western Australia, Perth, 106 p.

Lehane, B.M., Schneider, J.A., and Xu, X. (2005b). "The UWA-05 method for prediction of axial capacity of driven piles in sand." Frontiers in Offshore Geomechanics, (Proc. ISFOG-Perth), Taylor & Francis, London, 683–689.

Mayne, P.W. (2005). "Integrated ground behavior: In situ and laboratory tests." Deformation Characteristics of Geomaterials, Vol. 2 (Proc. Lyon, France), Taylor & Francis, London, 155 – 177.

Mayne, P.W. (2006). "Undisturbed sand strength from seismic cone tests." The 2nd James K. Mitchell Lecture, Geomechanics and Geoengineering, 1(4), 239 – 247.

Mayne, P.W. (2007). "Cone penetration testing – a synthesis of highway practice." NCHRP Synthesis 368, Transportation Research Board, National Academies Press, Washington, D.C., 117p.

Mayne, P.W., Coop, M.R., Springman, S.M., Huang, A., and Zornberg, J.G. (2009). "Geomaterials behavior and testing." Proc. 17th International Conference on Soil Mechanics & Geotechnical Engrg., Alexandria, Millpress-IOS Press, Rotterdam, Vol. 4, 2777 – 2872.

Mayne P.W., Peuchen, J., and Bouwmeester, D. (2010). "Estimation of soil unit weight from CPTs." Proc. 2nd International Symposium on Cone Penetration Testing, (CPT'10, Huntington Beach, CA), Vol 2, 169-176.

Poulos, H.G., and Davis, E.H. (1980). Pile Foundation Analysis and Design. John Wiley & Sons, NY, 397p.

Randolph, M.F. (2003). PIGLET: "Analysis and design of pile groups." Users' Manual, Ver. 4 – 2. Univ. of Western Australia, Perth.

Randolph, M.F., and Wroth, C.P. (1978). "Analysis of deformation of vertically-loaded piles." ASCE J. of the Geotechnical Engrg. Division, 104 (GT12), 1465 – 1488.

Randolph, M.F., and Wroth, C.P. (1979). "A simple approach to pile design and the evaluation of pile tests." Behavior of Deep Foundations, STP 670, ASTM, West Conshohocken, PA, 484 – 499.

Schneider, J.A., and Lehane, B.M. (2005). "Correlations for shaft capacity of offshore piles in sand." Frontiers in Offshore Geotechnics (Proc., ISFOG, Perth), Taylor & Francis, London, 757 – 763.

Schneider, J.A., Xu, X., and Lehane, B.M. (2008). "Database assessment of CPT-based design methods for axial capacity of driven piles in siliceous sands." J. of Geotechnical and Geoenvironmental Engrg., 134(9), 1227 – 1244.

Senneset, K., Sandven, R., and Janbu, N. (1989). "Evaluation of soil parameters from piezocone tests." Transportation Research Record 1235, National Research Council, Washington, D.C., 24 – 37.

Takesue, K., Sasao, H., and Matsumoto, T. (1998). "Correlation between ultimate pile skin friction and CPT data." Geotechnical Site Characterization, Vol. 2 (Proc. ISC-1, Atlanta), Balkema, Rotterdam, 1177 – 1182.

Timoshenko, S.P., and Goodier, J.N. (1951). Theory of Elasticity. McGraw-Hill Book Co., NY, 506p.

Vesic´, A.S. (1977). "Design of pile foundations." NCHRP Synthesis of Highway Practice 42, Transportation Research Board, National Research Council, Washington, D.C., 68p.

Zuidberg H.M., and Vergobbi P. (1996). "EURIPIDES, load tests on large driven piles in dense silica sands." Proc. 28th Offshore Technology Conference, Houston, Texas, Vol. 1, 193 – 206.

INTERNATIONAL JOURNAL OF GEOENGINEERING CASE HISTORIES

The Journal's Open Access Mission is generously supported by the following Organizations:

dar

Geosyntec▷
consultants

engineers | scientists | innovators

CONETEC

MUD BAY DRILLING   LANKELMA   Geotech DRILLING

ENGEO
Expect Excellence